

SUPPLEMENTARY FIGURES

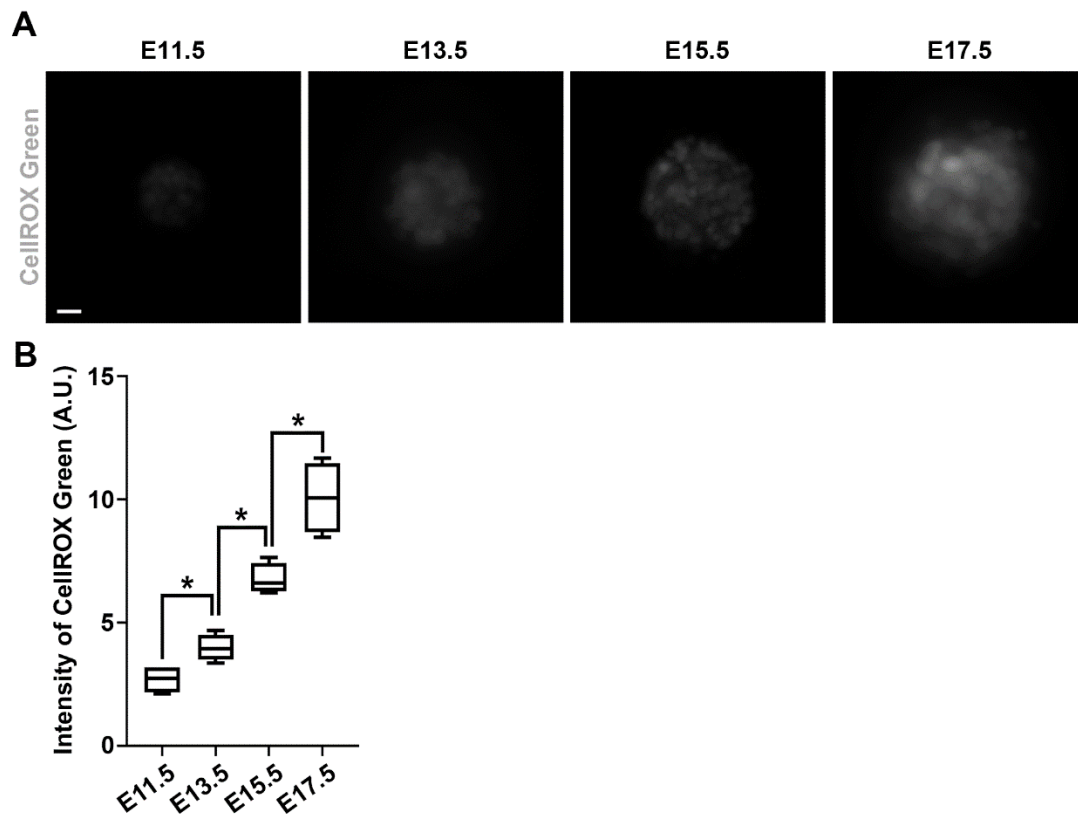


Figure S1: Progressive increase in oxidative stress in the VZ of the developing mouse cortex.

(A) Representative images of E11.5, E13.5, E15.5, and E17.5 neurospheres stained for CellROX Green (gray). Scale bars: 10 μ m. (B) Quantification of the ROS level in individual neurospheres prepared at different embryonic stages (A.U.). n = 4 for each embryonic stage; *, P < 0.05.

For box-whisker plots: center line, median; box, interquartile range; whiskers, minimum and maximum. Statistical analysis was performed using unpaired Student's t-test. Similar plot and statistical analysis were used in subsequent figures.

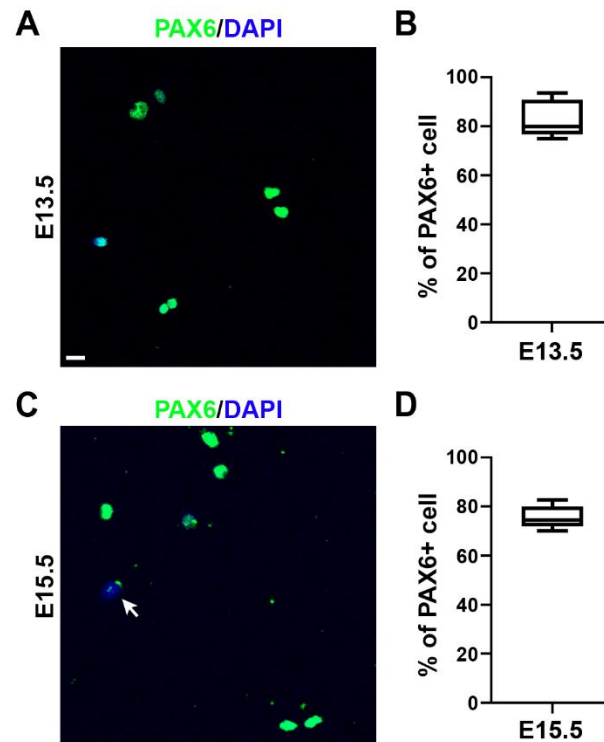


Figure S2: Dissected cortical VZ tissues contain predominantly RGPs. (A, C) Representative images of E13.5 (A) and E15.5 (C) dissociated cell culture of the cortical VZ tissues stained for PAX6 (green) and with DAPI (blue). Arrow indicate Pax6⁻/DAPI⁺ cells. Scale bars: 10 μ m. (B, D) Quantification of the percentage of PAX6⁺ RGPs among the total cells in culture at E13.5 (B) and E15.5 (D). n = 4 brains for each embryonic stage. *, P < 0.05.

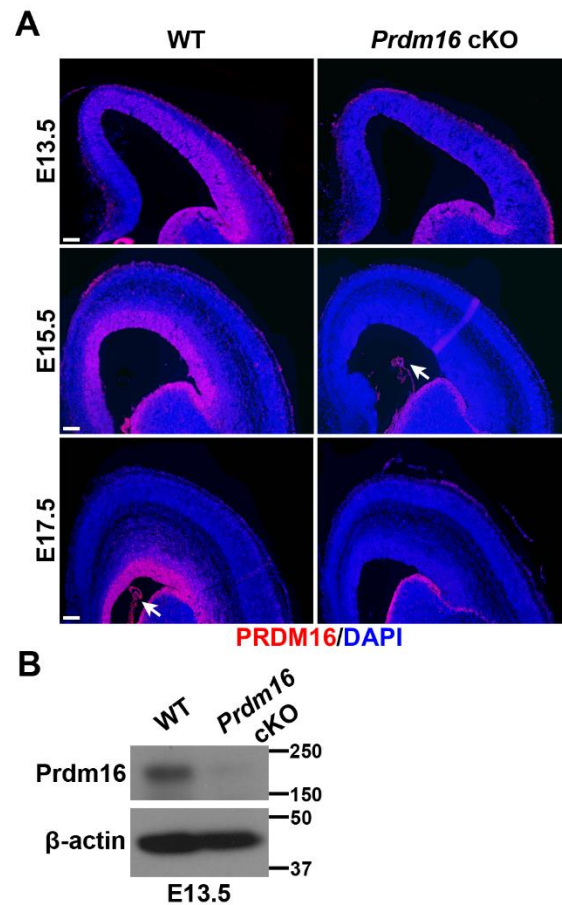


Figure S3: Selective removal of PRDM16 in RGPs. (A) Representative images of E13.5, E15.5, and E17.5 WT and *Prdm16* cKO cortices stained for PRDM16 (red) and with DAPI (blue). Arrows indicate expression of PRDM16 in the choroid plexus. Scale bars: 0.5mm. (B) Western blot assay of PRDM16 expression in E13.5 WT and *Prdm16* cKO cortices. Note that the expression of PRDM16 is largely abolished in the *Prdm16* cKO cortex.

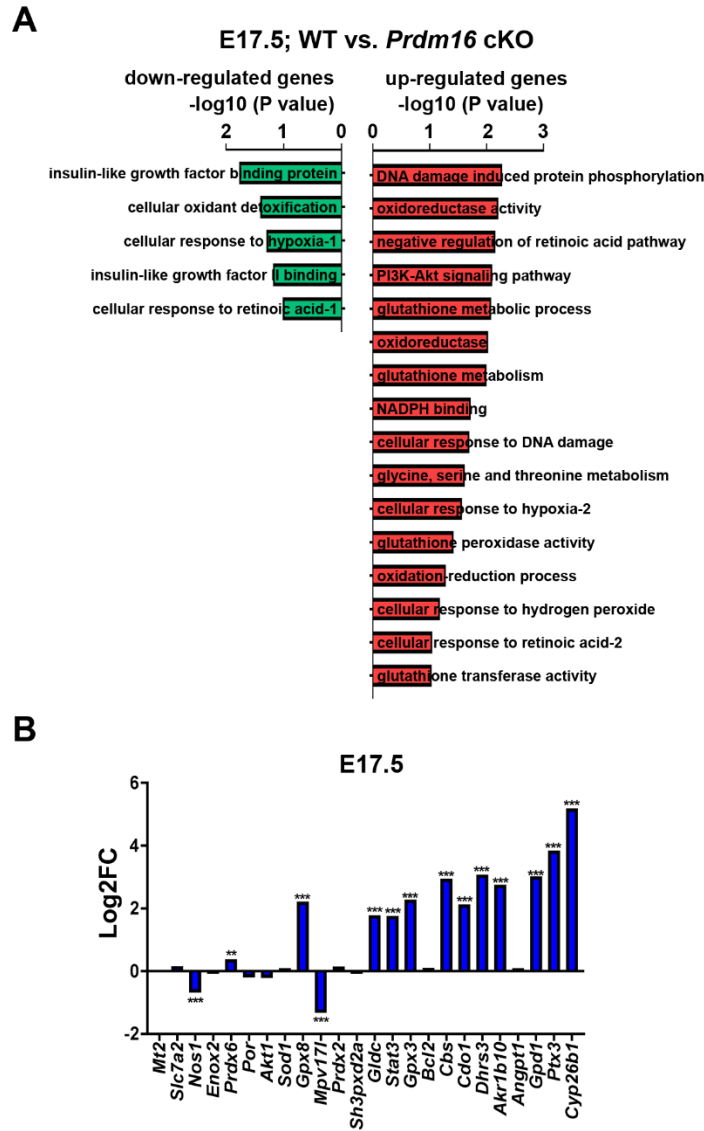


Figure S4: PRDM16 removal causes drastic changes in oxidative stress responsive gene sets.

(A) GSEA of the RNA-seq data from E17.5 WT and *Prdm16* cKO VZ tissues reveals the drastic changes in ROS pathway gene sets. Down-regulated gene sets in *Prdm16* cKO versus WT are in green and up-regulated gene sets in red. Cutoff: P value < 0.05. (B) Quantification of the changes in the expression level of ROS related genes in E17.5 *Prdm16* cKO VZ compared with the WT. WT, n = 3 brains; *Prdm16* cKO, n = 3 brains; ***, P < 0.005; **, P < 0.01.

For bar chart, data is shown as mean + SEM. Statistical analysis was performed with unpaired Student's t-test. Similar plot and statistical analysis were used in subsequent figures.

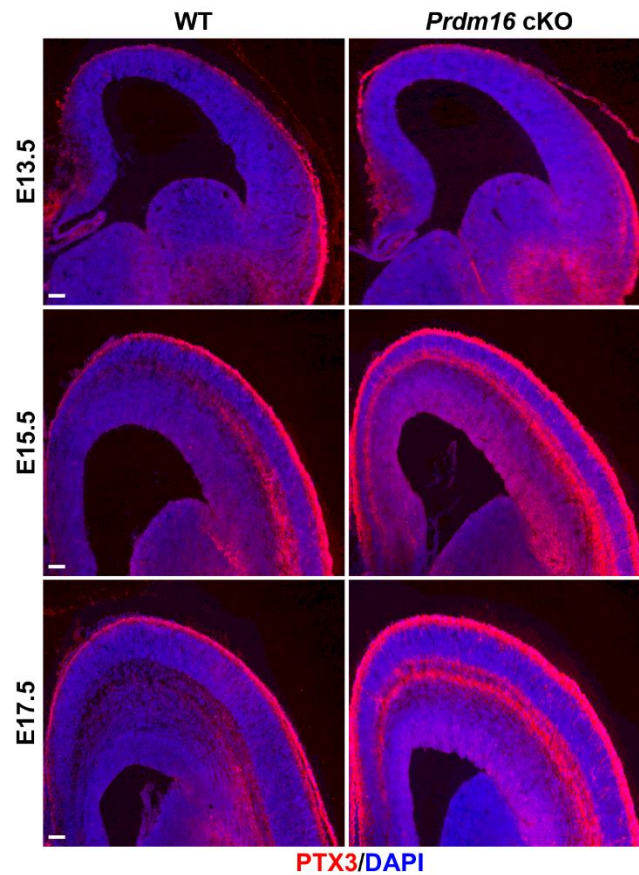


Figure S5: PRDM16 removal leads to a progressive increase in oxidative stress responsive gene *Ptx3* expression. Representative images of control WT and *Prdm16* cKO cortices stained for PTX3 (red) and with DAPI (blue) at different embryonic stages. Scale bars: 0.5 mm.

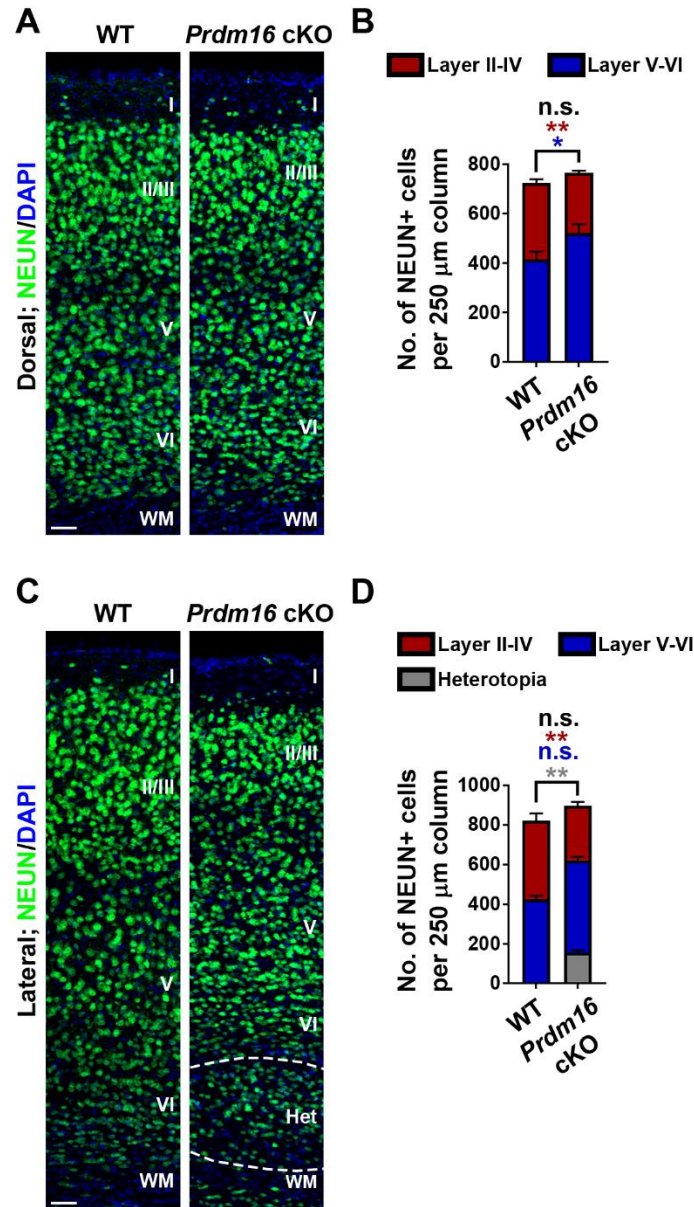


Figure S6: Deletion of *Prdm16* affects the density and composition of superficial and deep-

layer neurons (A) Representative images of the dorsal region of P21 WT and *Prdm16* cKO

cortices stained for NEUN (green) and with DAPI (blue). Scale bar: 200 μ m. **(B)** Quantification

of the numbers of NEUN⁺ neurons per 250 μ m column in A. WT, n = 3 brains; *Prdm16* cKO, n =

3 brains. **, P < 0.01; *, P < 0.05; n.s., not significant. **(C)** Representative images of the lateral

region of P21 WT and *Prdm16* cKO cortices stained for NEUN (green) and with DAPI (blue).

Scale bar: 200 μ m. **(D)** Quantification of the numbers of NEUN⁺ neurons per 250 μ m column in

C. WT, n = 3 brains; *Prdm16* cKO, n = 3 brains. **, P < 0.01; *, P < 0.05; n.s., not significant.

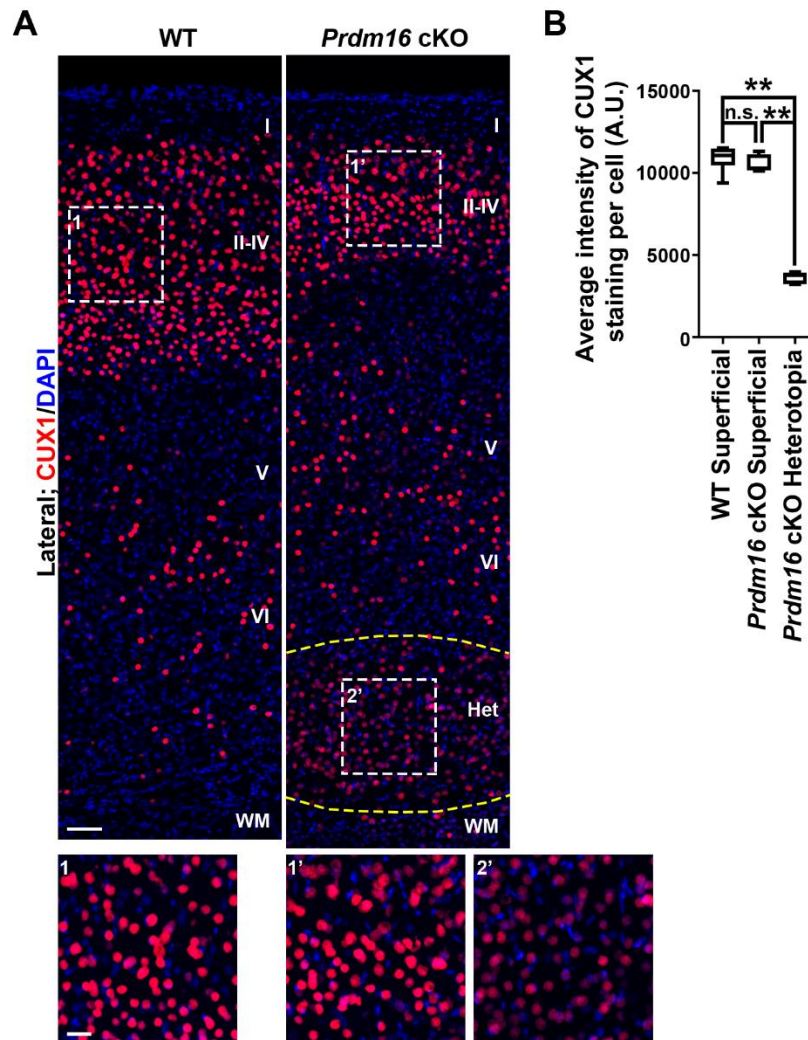


Figure S7: Weak expression of superficial neuron marker CUX1 in heterotopia neurons. (A) Representative images of P21 WT and *Prdm16* cKO cortices stained for CUX1 (red) and DAPI (blue). High magnification images of normal superficial layer neurons (area 1 and 1') and heterotopia neurons (area 2') are shown at the bottom. Scale bar: 200 μ m and 50 μ m. **(B)** Quantification of CUX1 expression level in individual normal superficial layer neurons and heterotopia neurons (A.U.). WT, n = 4 brains; *Prdm16* cKO, n = 4 brains. **, $P < 0.01$; n.s., not significant.

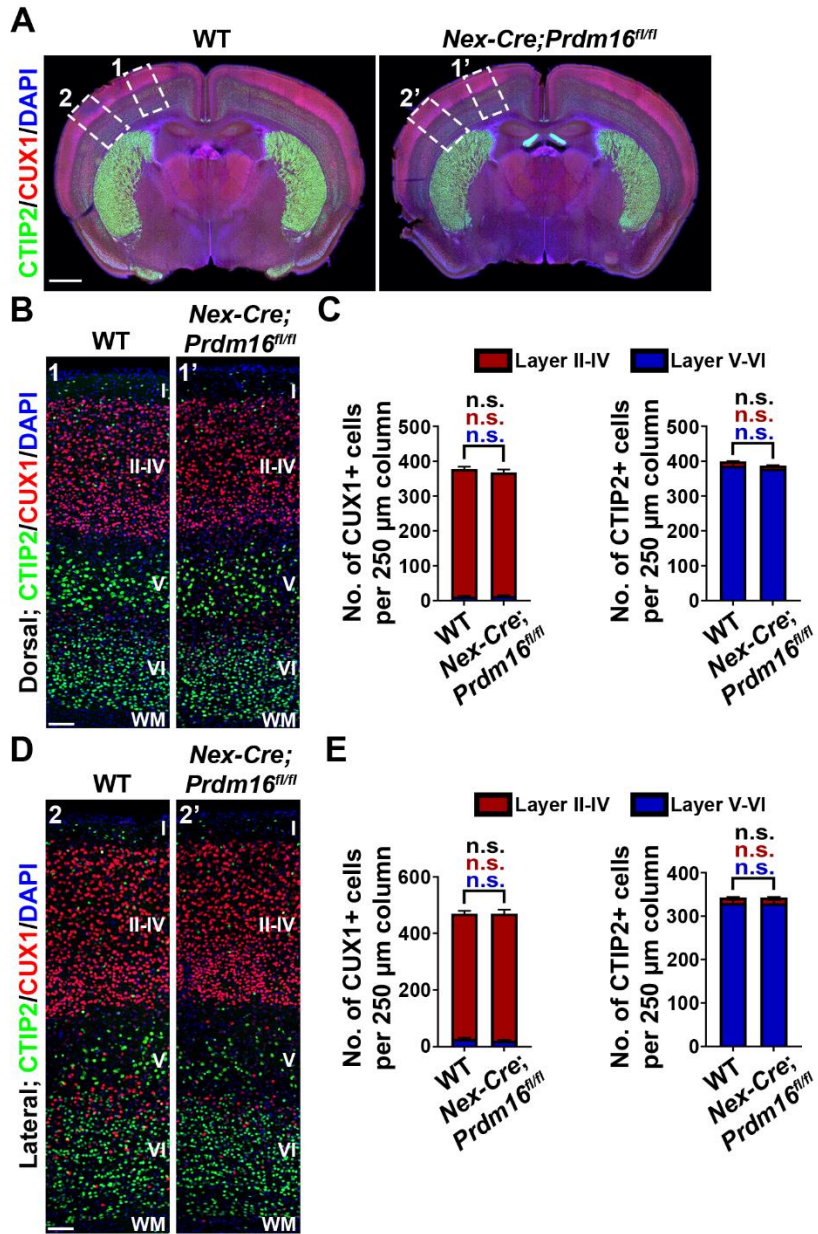


Figure S8: *Prdm16* deletion in postmitotic neurons does not cause any obvious defects in cortical neurogenesis and neuronal organization. (A) Representative images of P21 WT and *Nex-Cre;Prdm16^{fl/fl}* brain cortices stained for CUX1 (red) and CTIP2 (green), and with DAPI (blue). White broken rectangles indicate dorsal (1 and 1') and lateral (2 and 2') regions of the cortex shown in B and D, respectively. Scale bar: 1 mm. (B) Representative images of the dorsal region of P21 WT and *Nex-Cre;Prdm16^{fl/fl}* brain cortices stained for CUX1 (red) and CTIP2 (green), and with DAPI (blue). Scale bar: 200 μ m. (C) Quantification of the number of CUX1⁺ (top) and CTIP2⁺ (bottom) neurons per 250 μ m column. WT, n = 3 brains; *Nex-Cre;Prdm16^{fl/fl}*, n = 3 brains. n.s., not significant. (D) Representative images of the lateral region of P21 WT and *Nex-Cre;Prdm16^{fl/fl}* brain cortices stained for CUX1 (red) and CTIP2 (green), and with DAPI (blue). Scale bar: 200 μ m. (E) Quantification of the number of CUX1⁺ (top) and CTIP2⁺ (bottom) neurons per 250 μ m column. WT, n = 3 brains; *Nex-Cre;Prdm16^{fl/fl}*, n = 3 brains. n.s., not significant.

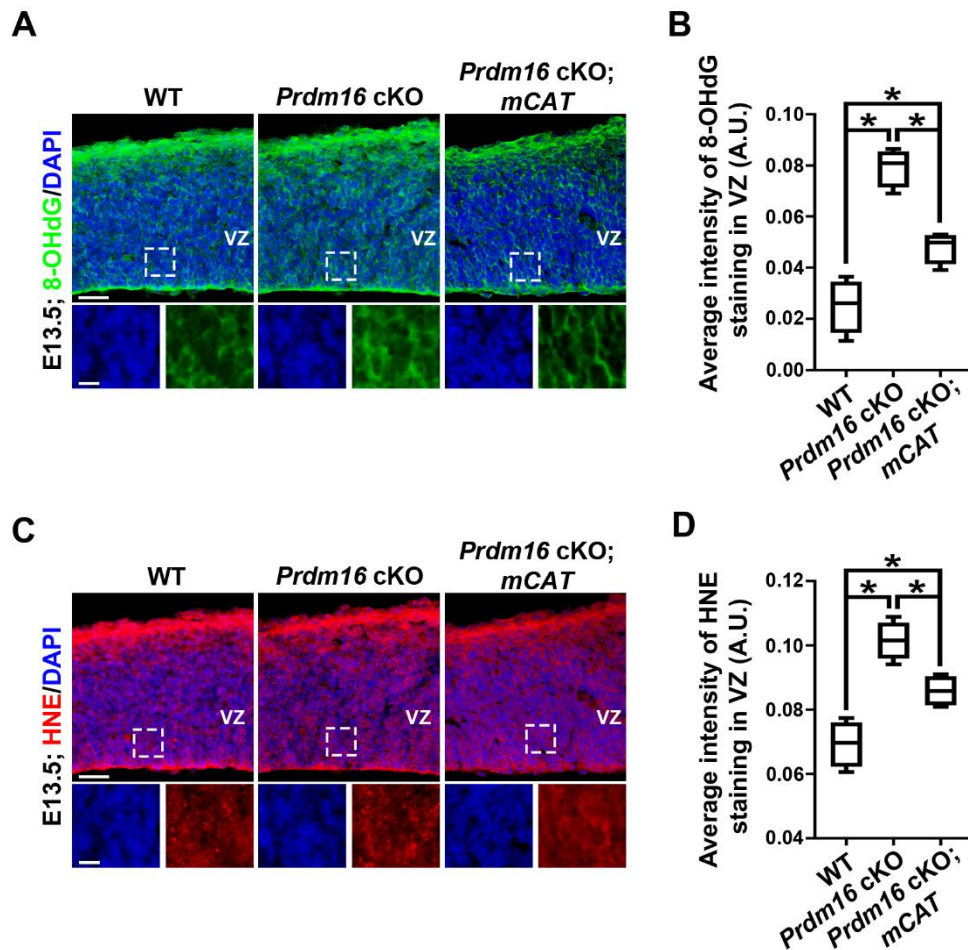


Figure S9: PRDM16 removal leads to an increase in oxidative stress E13.5. (A) Representative images of the dorsal region of E13.5 WT, *Prdm16* cKO, and *Prdm16* cKO;*mCAT* cortices stained for 8-OHdG (green) and with DAPI (blue). High magnification images of the VZ (broken lines) are shown at the bottom. Scale bars: 50 μ m and 20 μ m. (B) Quantification of the 8-OHdG expression level in the VZ (A.U.). WT, n = 4 brains; *Prdm16* cKO, n = 4 brains; *Prdm16* cKO;*mCAT*, n = 4 brains. *, P < 0.05. (C) Representative images of the dorsal region of E13.5 WT, *Prdm16* cKO and *Prdm16* cKO;*mCAT* cortices stained for HNE (red) and with DAPI (blue). High magnification images of the VZ (broken lines) are shown at the bottom. Scale bars: 50 μ m and 20 μ m. (D) Quantification of the HNE expression level in the VZ (A.U.). WT, n = 4 brains; *Prdm16* cKO, n = 4 brains; *Prdm16* cKO;*mCAT*, n = 4 brains. *, P < 0.05.

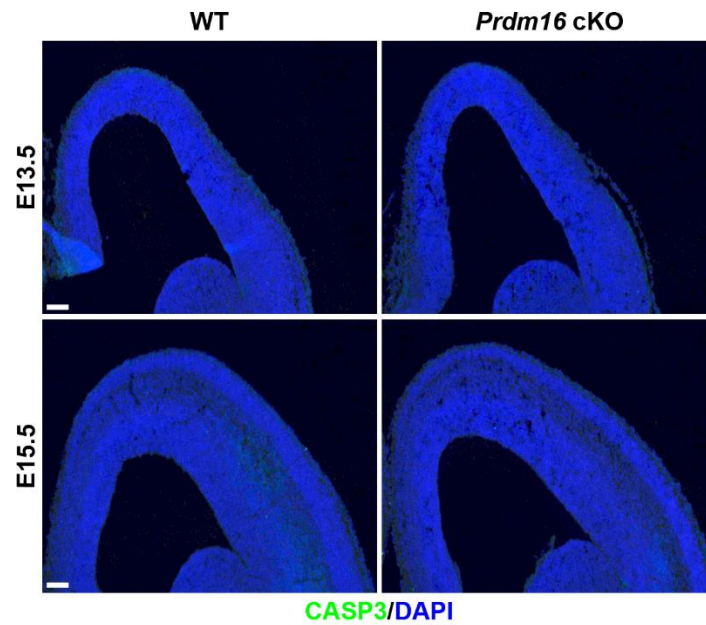


Figure S10: *Prdm16* deletion does not induce cell death at E13.5 or E15.5. Representative images of E13.5 and E15.5 WT and *Prdm16* cKO cortices stained for CASP3 (green) and with DAPI (blue). Scale bars: 0.5mm. Note no obvious increase in CASP3 staining in the *Prdm16* cKO cortex compared with the WT control.

SUPPLEMENTARY TABLES

Table S1: List of the top forty well-established genes known to regulate ROS with the cutoff P value < 0.05 that were used to perform GSEA for WT cortical VZ tissues. **(A)** E11.5 vs E13.5 **(B)** E13.5 vs E15.5 **(C)** E15.5 vs E17.5 **(D)** top 40 ROS related genes

[Click here to Download Table S1](#)

Table S2: List of top 500 differentially expressed genes used in the GSEA between WT and *Prdm16* cKO cortical VZ tissues at **(A)** E13.5, **(B)** E15.5, and **(C)** E17.5.

[Click here to Download Table S2](#)

Table S3: List of genes involved in cell migration among the top 500 differentially expressed genes in between WT and *Prdm16* cKO cortical VZ tissues at E13.5, E15.5, and E17.5. **(A)** Migration genes from Baizabal et al., 2018. **(B)** Migration genes among our top 500 differentially expressed genes.

[Click here to Download Table S3](#)